Nuclear Overhauser Effect Studies of the Conformations of MgATP Bound to the Active and Secondary Sites of Muscle Pyruvate Kinase†

Paul R. Rosevear*

Department of Biochemistry and Molecular Biology, University of Texas Medical School at Houston, Houston, Texas 77025

Terry L. Fox and Albert S. Mildvan

Department of Biological Chemistry, The Johns Hopkins University School of Medicine, Baltimore, Maryland 21205

Received December 3, 1986; Revised Manuscript Received February 11, 1987

ABSTRACT: MgATP binds both at the active site (site 1) and at a secondary site (site 2) on each monomer of muscle pyruvate kinase as previously found by binding studies and by X-ray analysis. Interproton distances on MgATP bound at each site have been measured by the time-dependent nuclear Overhauser effect in the absence and presence of phosphoenolpyruvate (P-enolpyruvate), which blocks ATP binding at site 1. Interproton distances at site 2 are consistent with a single conformation of bound ATP with a high anti-glycosidic torsional angle ($\chi = 68 \pm 10°$) and a C3′-endo ribose pucker ($\delta = 90 \pm 10°$). Interproton distances at site 1, determined in the absence of P-enolpyruvate by assuming the averaging of distances at both sites, cannot be fit by a single adenine–ribose conformation but require the contribution of at least three low-energy structures: 62 ± 10% low anti ($\chi = 30°$), C3′-endo; 20 ± 8% high anti ($\chi = 55°$), O1′-endo; and 18 ± 8% syn ($\chi = 217°$), C2′-endo. Although a different set of ATP conformations might also have fit the interproton distances, the mixture of conformations used also fits previously determined distances from Mn^{2+} to the protons of ATP bound at site 1 [Sloan, D. L., & Mildvan, A. S. (1976) *J. Biol. Chem. 251*, 2412] and is similar to the adenine–ribose portion of free $Co(NH_3)_4ATP$, which consists of 35% low anti, 51% high anti, and 14% syn [Rosevear, P. R., Bramson, H. N., O'Brian, C., Kaiser, E. T., & Mildvan, A. S. (1983) *Biochemistry 22*, 3439]. The unusual multiplicity of adenine–ribose conformations of ATP bound at the active site of pyruvate kinase is consistent with the low specificity of this enzyme for nucleotide substrates [Plowman, K. M., & Krall, A. R. (1965) *Biochemistry 4*, 2809] and with the high mobility of bound 1,N^6-ethenoadenosine 5′-triphosphate [Barrio, J. R., Secrist, J. A., Chien, Y., Taylor, P. J., Robinson, J. L., & Leonard, N. J. (1973) *FEBS Lett. 29*, 215].

NMR methods have been widely used to determine the conformations and arrangement of enzyme-bound flexible substrates such as ATP (Sloan & Mildvan, 1976; Granot et al., 1979; Rosevear et al., 1983). Two NMR approaches especially useful for these purposes are the paramagnetic probe–T_1 method, which is used to measure metal–nucleus distances (Mildvan & Gupta, 1978; Mildvan et al., 1980), and the nuclear Overhauser effect, which is used to measure relative and absolute interproton distances (Noggle & Schirmer, 1971; Tropp & Redfield, 1981; Mildvan et al., 1983). The applications of both methods have yielded mutually consistent conformations of ATP on protein kinase, of AMP on adenylate kinase, and of TTP and dATP on DNA polymerase, indicating unique nucleotide conformations on these enzymes (Granot et al., 1979; Rosevear et al., 1983; Fry et al., 1985; Ferrin & Mildvan, 1985, 1986).

Pyruvate kinase has long been known to have two nucleotide binding sites per subunit as determined by binding studies (Mildvan & Cohn, 1966) and by X-ray crystallography (Stuart et al., 1979). At the active site (site 1), metal–ATP complexes bind competitively with respect to phosphoenolpyruvate (P-enolpyruvate)[1] as detected by steady-state kinetics (Reynard et al., 1961; Mildvan & Cohn, 1966) and NMR measurements (Melamud & Mildvan, 1975; Sloan & Mildvan, 1976). Site 1 also contains a tight divalent cation binding site, the occupancy of which is essential for activity (Mildvan & Cohn, 1965). An ATP binding site with these properties has been found by X-ray analysis to be located between the A and B domains of each monomer of this tetrameric enzyme (Stuart et al., 1979).

A second and somewhat weaker nucleotide binding site (site 2), which has no known function, has been detected by binding studies (Mildvan & Cohn, 1966) and has been located by X-ray analysis to be between the A and C domains of each subunit, ~30 Å from site 1 (Stuart et al., 1979).

At the active site, site 1, distances measured from enzyme-bound Mn^{2+} to three protons and to the three phosphorus atoms of ATP were consistent with a highly extended nucleotide conformation (Sloan & Mildvan, 1976). However, these data, while selective for site 1, gave no information on the uniqueness of the ATP conformation at the active site.

To examine this question, an independent study, using the NOE method, has been made to determine the conformation of ATP bound at site 1. The use of the NOE method at site 1 is, however, complicated by the presence of site 2, since the interproton cross-relaxation rates of ATP exchanging into both sites are averaged. To deal with this problem, we have initially determined the interproton distances and conformation of MgATP bound only at site 2 by saturating the enzyme with

† This work was supported by National Institutes of Health Grant AM28616.

[1] Abbreviations: ε-ATP, 1,N^6-ethenoadenosine 5′-triphosphate; DSS, sodium 4,4-dimethyl-4-silapentanesulfonate; P-enolpyruvate (PEP), phosphoenolpyruvate; NOE, nuclear Overhauser effect; Tris, tris(hydroxymethyl)aminomethane; SDS, sodium dodecyl sulfate; FID, free induction decay.

0006-2960/87/0426-3487$01.50/0

P-enolpyruvate, preventing MgATP binding at site 1. We next determined the average interproton distances in MgATP bound at both site 1 and site 2 by NOE measurements in the absence of P-enolpyruvate. The average interproton distances at both sites, together with those measured only at site 2, permitted us to determine the interproton distances and conformation of MgATP at site 1. The ATP conformation at the active site thus determined was found to be consistent with the distances from Mn^{2+} to ATP measured independently by the paramagnetic probe–T_1 method. A preliminary report of this work has been published (Rosevear et al., 1986).

Experimental Procedures

Materials. Tris, ATP, ADP, PEP, NADH, Sephadex G25, Sephadex G200, and lactate dehydrogenase were purchased from Sigma. Rabbit muscle pyruvate kinase used in this study was obtained from Boehringer. The ammonium sulfate was removed by gel filtration using Sephadex G25. When assayed according to the coupled lactate dehydrogenase reaction (Bücher & Pfleiderer, 1955), the specific activity of the commercial pyruvate kinase was routinely between 200 and 230 units/mg.

Methods. Pyruvate kinase (130 mg) was further purified on a 2.5 × 48 cm Sephadex G200 column equilibrated with 10 mM Tris–HCl at pH 7.5 and 100 mM KCl to remove an ATPase contaminant. The specific activity of pyruvate kinase eluting from the column was routinely found to be 270–310 units/mg. SDS–polyacrylamide gel electrophoresis of the enzyme gave a single band. The concentration of pyruvate kinase was determined spectrophotometrically by using $A^{1\%}_{280nm}$ = 5.4, assuming a subunit molecular weight of 59 300 (Steinmetz & Deal, 1966). The enzyme was concentrated and deuteriated in a collodion bag by repeated vacuum dialysis at 4 °C. Solutions used in the NMR experiments contained 10 mM deuteriated Tris–HCl buffer, pH 7.4, and 100 mM KCl. The typical NMR experiment contained rabbit muscle pyruvate kinase (0.70–1.0 mM subunit), ATP (7–10 mM), and $MgCl_2$ (14–16 mM) in a total volume of 0.4 mL. When needed, P-enolpyruvate was used at a saturating concentration (37 mM) to block ATP binding at the catalytic site. The addition of 3.5 M guanidinium chloride, which was found to be sufficient to denature the protein, removed all of the negative NOEs observed. No positive NOEs were observed under any of the experimental conditions used in this study.

^1H NMR spectra were obtained on a Bruker WM 250 NMR spectrometer using 16-bit A/D conversion. Chemical shifts were relative to external DSS. The time dependence of the nuclear Overhauser effect was measured by using the following pulse sequence: {[RD–preirradiate (t,ω_1)–observation pulse]$_{16}$–(RD–preirradiate $(t,\omega_{off\text{-}res})$–observation pulse]$_{16}$–[RD–preirradiate (t,ω_2)–observation pulse]$_{16}$} where RD is the relaxation delay, t is the duration of preirradiation, and ω is the frequency of the irradiated resonance. To ensure complete relaxation of the proton resonances between observation pulses, a relaxation delay $\geq 5T_1$ was routinely used. The proton decoupler was utilized to produce a selective preirradiation pulse of desired duration, t, usually between 50 and 600 ms. The NOE was observed by subtraction of the control FID from the experimental FID, and the difference FID was Fourier transformed and phased to give negative peaks for negative NOEs. The magnitude of the NOE was determined either by peak height measurement or by peak integration, which gave indistinguishable results (Rosevear et al., 1983).

The ribose H2′ resonance of ATP was obscured by the HDO signal and could not be directly observed in the presence of pyruvate kinase. The chemical shift of the ribose H2′ resonance was therefore determined by searching for a frequency which, upon preirradiation, gave a negative NOE to the ribose H1′ resonance. The chemical shift of the ribose H2′ obtained by this approach was found to be the same as the chemical shift of ribose H2′ in free MgATP. X-ray and model-building studies indicate that the ribose H1′ to H2′ distance lies within the limits of 2.9 ± 0.2 Å regardless of the ribose conformation or the glycosyl torsional angle (DeLeeuw et al., 1980; Levitt & Warshell, 1978; Rosevear et al., 1983). Thus, regardless of the conformations of ATP bound to pyruvate kinase, a negative NOE is always expected between these two protons.

Longitudinal relaxation rates $(1/T_1)$ were measured by selective saturation of individual resonances and monitoring their recoveries (Tropp & Redfield, 1981). Transverse relaxation rates $(1/T_2)$ were calculated from the line width at half-height $(\Delta\nu)$ by using the relation $1/T_2 = \pi\Delta\nu$.

Internuclear NOEs on bound MgATP were measured by selectively preirradiating the H1′, H2′, H3′, H4′, H5′, H5″, and H8 protons at varying times and observing the time-dependent changes in the magnetization of the monitored MgATP resonances. This approach allows discrimination between primary and secondary effects, since the latter display a long lag period before development of the NOE. The magnitude of the final steady-state NOE from spin B to spin A will depend on the competition between σ_{AB}, the cross-relaxation rate or the rate at which energy is transferred from spin B to spin A, and ρ_A, the spin–lattice relaxation rate. As previously shown (Wagner & Wüthrich, 1979; Rosevear et al., 1983) for a two-spin system, the cross-relaxation rate (σ_{AB}) can be calculated from the time dependence of the NOE and the selective longitudinal relaxation rate of spin A (ρ_A) by using eq 1 in which $f_A(B)_t$ is the NOE from spin A upon preirradiation of spin B for time t and c is the rate constant for saturation of spin B which is approximated by $^1/_2(1/T_{1B} + 1/T_{2B})$. The time dependence of the NOEs from each of the selectively preirradiated protons to the observed protons was fit with eq 1 by nonlinear regression analysis using the experimentally determined $f_A(B)_t$ and ρ_A values and varying both σ_{AB} and c. Values of c were found to vary between 7.5 and 19.1 s^{-1}. The calculated cross-relaxation rates (σ_{AB}) and the correlation functions $[f(\tau_r)]$ were used to calculate the distance between nuclei A and B (r_{AB}) by using eq 2 where the constant,

$$f_A(B)_t = \frac{\sigma_{AB}}{\rho_A}(1 - e^{-\rho_A t}) + \frac{\sigma_{AB}}{\rho_A - c}(e^{-\rho_A t} - e^{-t}) \qquad (1)$$

$$r_{AB} = D\left[\frac{f(\tau_r)}{\sigma_{AB}}\right]^{1/6} \qquad (2)$$

D, $(\gamma^4\hbar^2/10)^{1/6}$, is numerically equal to 62.02 Å $s^{-1/3}$ if A and B are protons. The correlation function $f(\tau_r)$ is given by eq 3 where ω_I is the nuclear precession frequency and τ_r is the correlation time. Equations 2 and 3 assume isotropic rotation of the molecule as a whole with a time constant τ_r shorter than any time constants of internal motion (Kalk & Berendsen, 1976). This approximation was justified by the results. The correlation time was calculated by assuming a fixed distance, independent of conformation, of 2.9 ± 0.2 Å between ribose H1′ and H2′ (Rosevear et al., 1983). Use of a single correlation time to calculate all internuclear distances makes the assumption that all internuclear vectors in ATP have the same correlation time as that found between ribose H1′ and H2′.

$$f(\tau_r) = \frac{6\tau_r}{1 + 4\omega_I^2\tau_r^2} - \tau_r \qquad (3)$$

RESULTS

Intramolecular NOEs on Enzyme-Bound MgATP. Figure 1A illustrates the negative interproton NOEs, observed on preirradiation of ribose H2′, to H1′ and to adenine H8 of MgATP (7.2 mM) exchanging into both nucleotide binding sites of rabbit muscle pyruvate kinase (0.81 mM). The NOE from H2′ to adenine H8 suggests an anti conformation for bound ATP. However, an NOE is also detected from H1′ to adenine H8 (Figure 1B) and, inversely, from adenine H8 to H1′ (Figure 1C) indicative of a syn conformation. Making use of the observation that site 1 has a 22-fold higher affinity for ADP than does site 2 (Mildvan & Cohn, 1966), it is estimated that site 1 is 98% occupied while site 2 is 68% occupied with nucleotide under these conditions. Figure 1D–F illustrates the corresponding NOEs observed under otherwise identical conditions except for the presence of 37 mM P-enolpyruvate, which competitively blocks the binding of MgATP at site 1 (Reynard et al., 1961; Mildvan & Cohn, 1966; Melamud & Mildvan, 1975; Sloan & Mildvan, 1976).[2] Hence, the negative NOEs observed in the presence of P-enolpyruvate result from the binding of MgATP only at site 2. While the anti conformation persists, as indicated by the NOE from H2′ to H8 (Figure 1C), a syn conformation is no longer detected, as revealed by the loss of the NOEs from H1′ to H8 (Figure 1E) and from H8 to H1′ (Figure 1F).

Both in the absence and in the presence of P-enolpyruvate, the magnitude of the NOE as a function of preirradiation time was measured to distinguish primary NOEs from higher order effects and spin diffusion (Figure 2). In all cases, the time dependence of the NOEs could be fit by the simple two-spin equation (eq 1), using the separately measured longitudinal relaxation rates of the protons receiving the NOEs (Table I). When MgATP is bound only at site 2 (Figure 2A,B, Table I), strong NOEs are seen from H2′ and H3′ of ribose to adenine H8 (σ = −0.642 and −0.289 s^{-1}) while no NOE is detected from H1′ to H8 ($\sigma \geq -0.06$ s^{-1}), indicative of an anti conformation. In the absence of P-enolpyruvate, when both sites 1 and 2 are occupied, NOEs are observed not only from H2′, H3′ and H5, H5″ but also from H1′ to adenine H8 (Figure 2A,B,D, Table I). The latter and its inverse, the NOE from H8 to H1′ (Figure 2E), indicate both syn and anti nucleotide conformations when MgATP binds at both sites.

Determination of Average Interproton Distances on Enzyme-Bound MgATP. The cross-relaxation rates (σ) and longitudinal relaxation rates (ρ) used to fit the data of Figure 2 are given in Table I, together with the transverse relaxation rates ($1/T_2$) of the H1′ and H8 protons of MgATP. The $1/T_2$ values, which set lower limits on the exchange rates of MgATP from its enzyme complexes, exceed, by at least an order of magnitude, those of σ and ρ. Hence, the σ and ρ values are in fast exchange, averaging those of free and enzyme-bound MgATP. For distance calculations, a value of the correlation time τ_c is required. As discussed previously (Rosevear et al., 1983), the value of τ_c is obtained from the H2′ to H1′ cross-relaxation rate (Figure 2C, Table I) by setting the distance from H2′ to H1′ to be 2.90 Å. This distance has been found, by X-ray studies of many nucleotides and model building, to vary little (±0.2 Å) despite wide variations of ribose puckers (Rosevear et al., 1983). The interproton dis-

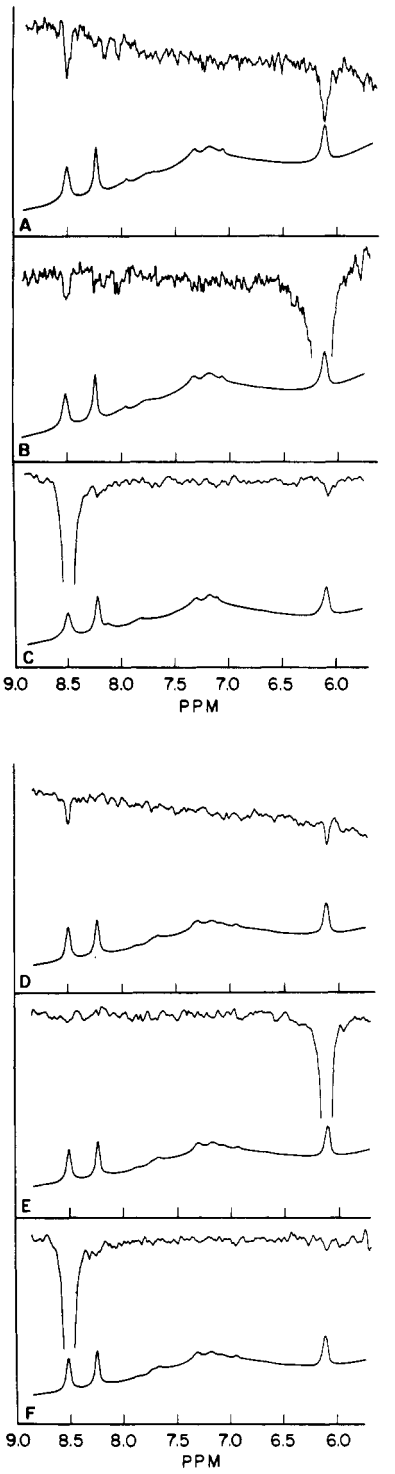

FIGURE 1: Proton NMR spectra of MgATP in the presence of pyruvate kinase, searching for interproton NOEs, and in the absence (A–C) or presence of P-enolpyruvate (D–F) which blocks MgATP binding at site 1. All samples contained 7.2 mM ATP, 15.9 mM $MgCl_2$, 0.81 mM pyruvate kinase subunits, 100 mM KCl, and 10 mM deuteriated Tris-HCl, pH 7.5 (in ^2H_2O), and samples D–F contained, in addition, 37 mM P-enolpyruvate. Each panel shows a control spectrum (lower) obtained on preirradiation at 9.50 ppm for 0.10 s and a difference spectrum (upper), control minus test X64 (A, B), or control minus test X32 (C–F). The test spectra were obtained by preirradiation of H2′ at 4.73 ppm from DSS (A, D), H1′ at 6.11 ppm (B, E), or H8 at 8.49 ppm (C, F) for 0.10 s. NMR spectra were obtained at 250 MHz with 16-bit A/D conversion using a total of 256 transients, each of 4098 data points with a recycle time of 1.4 s, a spectral width of 3012 Hz, quadrature phase detection, a 90° pulse, and a decoupler power of 40 dB below 0.2 W. T = 24 °C. A line broadening of 2.0 Hz was used.

[2] Since the Mg^{2+} complex of pyruvate kinase has a 4.8-fold higher affinity for P-enolpyruvate than for ATP at site 1 under these conditions (Mildvan & Cohn, 1966), and since the concentration of P-enolpyruvate is 5.1-fold greater than that of ATP, it is estimated that 96% of the ATP bound at site 1 was displaced by P-enolpyruvate.

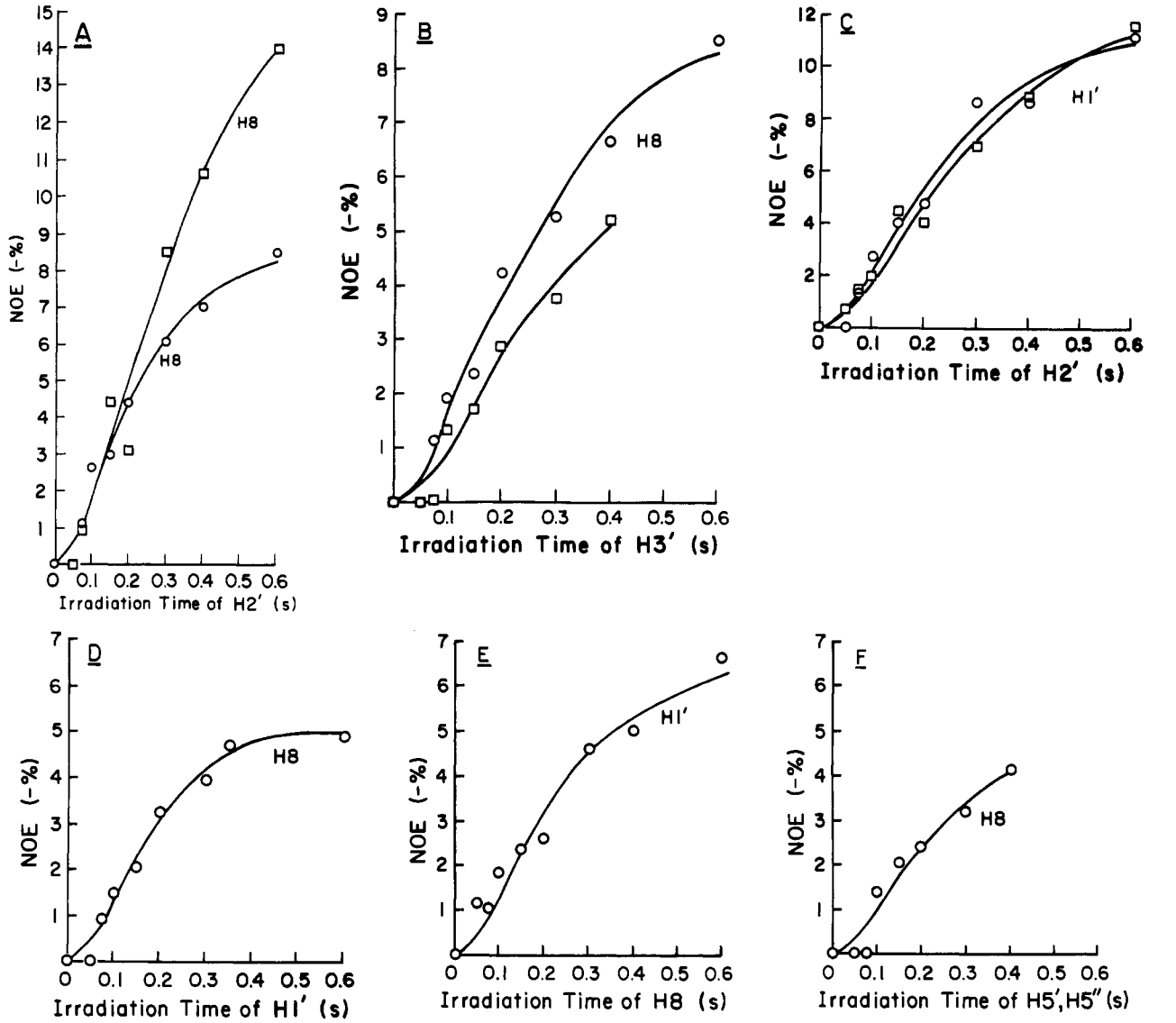

FIGURE 2: Time dependence of interproton NOEs in MgATP interacting with pyruvate kinase. Preirradiated and observed nuclei are as follows: (A) H2′ → H8; (B) H3′ → H8; (C) H2′ → H1′; (D) H1′ → H8; (E) H8 → H1′ [(○) MgATP; (□) MgATP + P-enolpyruvate]; (F) H5′, H5″ → H8 (MgATP + P-enolpyruvate). Solid curves represent theoretical fits to the data using eq 1 with the σ values given in Table I and c values ranging from 7.5 to 19.1 s^{-1}. Experimental conditions were as described in Figure 1.

Table I: Longitudinal Relaxation Rates, Cross-Relaxation Rates, and Interproton Distances on Pyruvate Kinase Bound MgATP[a]

proton pair (B → A)	MgATP				MgATP + PEP				
	ρ_A (s^{-1})	σ_{AB} (s^{-1})	$(1/T_2)_A$ (s^{-1})	$\langle r \rangle$ (Å)	ρ_A (s^{-1})	σ_{AB} (s^{-1})	$(1/T_2)_A$ (s^{-1})	r(site 2) (Å)	r(site 1)[b] (Å)
H1′ → AH8	8.33	0.424	38	3.22	3.70	≤0.060	24	≥4.26	2.96,[c] 2.99[d]
AH8 → H1′	6.90	0.457	40	3.18	4.65	≤0.060	37	≥4.26	2.92,[c] 2.95[d]
H2′ → AH8	8.33	0.714	38	2.96	3.70	0.642	24	2.87	3.03
H3′ → AH8	8.33	0.751	38	2.93	3.70	0.289	24	3.28	2.79
H5′,5″ → AH8	8.33	≤0.080	38	≥4.26	3.70	0.213	24	3.44	≥4.26
H2′ → H1′	6.90	0.800	40	2.90[e]	4.65	0.596	37	2.90[e]	2.90[e]

[a] Cross-relaxation rates obtained from the data of Figure 2. The errors in the relaxation rates are ±10%, in the relative distances are ±2%, and in the absolute distances are ±8%. [b] Derived from $\langle r \rangle$ and r(site 2) by using eq 4. [c] Assuming r(site 2) = ∞. [d] Assuming r(site 2) = 4.26 Å. [e] Assumed from X-ray data (2.9 ± 0.2 Å; Rosevear et al., 1983).

tances in MgATP bound at site 2 (r_2) and the average interproton distances at both sites 1 and 2 ($\langle r \rangle$), obtained from eq 4, are given in Table I. The corresponding interproton distances in MgATP bound at site 1 (r_1) (Table I) are calculated from

$$\langle r^{-6} \rangle = f_1(r_1)^{-6} + f_2(r_2)^{-6} \quad (4)$$

In eq 4, f_1 and f_2 are the fractional contributions of site 1 and site 2 to the average distance, estimated as 0.60 and 0.40, respectively, from the dissociation constants of ADP from both sites (Mildvan & Cohn, 1966). Because of the sixth root taken in such distance calculations, the ±20% uncertainty in the relative occupancies of sites 1 and 2 introduces a maximal error of only ±3% in r_1.

Conformation of Enzyme-Bound MgATP. Because of its relative simplicity, the conformation of MgATP bound at site 2, the secondary site, will be considered first. A model of the adenine–ribose portion of MgATP, based on the distances measured at site 2 (Table I), shows a high anti-glycosidic torsional angle (χ = 68 ± 10°) and a 3′-endo ribose pucker

Table II: Conformations Contributing to the Structure of MgATP Bound to Site 1 of Pyruvate Kinase[a]

conformation[a]			distances (Å)[b]						
			from adenine H8 to ribose			from Mn^{2+} to ATP[c]			
name	glycosidic torsional angle (deg)	ribose pucker	H1′	H2′	H3	H1′	H2	H8	fractional population[d]
I	30	3′-endo	3.8	3.9	2.5	7.5	9.1	6.0	0.62 ± 0.10
II	55	O1′-endo	3.8	2.4	3.2	7.3	8.7	7.3	0.20 ± 0.08
III	217	C2′-endo	2.3	3.7	5.6	7.6	7.3	7.3	0.18 ± 0.08
$\langle r \rangle_{calcd}$[e,f]			2.96	3.03	2.68	7.47	8.45	6.31	
$\langle r \rangle_{obsd}$[g,h]			2.96 ± 0.24	3.03 ± 0.24	2.79 ± 0.22	7.5 ± 0.8	9.1 ± 1.0	6.0 ± 0.6	

[a] Conformations were chosen on the basis of those most frequently found by crystallographic analysis and predicted by theoretical studies to be at or near an energy minimum (deLeeuw et al., 1980; Berthod & Pullman, 1973; Yathindra & Sundaralingam, 1973). [b] Distances (±0.1 Å) determined by model building for the indicated glycosidic torsional angles and ribose puckers. [c] Distances within each individual conformation were measured by placing the Mn^{2+} atom 5.1, 5.0, and 4.9 Å from each of the three phosphorus atoms of ATP (Sloan & Mildvan, 1976). [d] Fractional populations of the three conformations of MgATP were calculated from simultaneous eq 5–8 using the theoretical interproton distances in each conformation and the experimentally determined interproton distances at site 1 as determined by the NOE method (Table I). [e] Calculated and observed interproton distances were constrained to agree, with experimental error, by using eq 5–8 to determine the fractional populations. [f] Calculated Mn^{2+}–proton distances are based on theoretical distances determined by model building of conformations I–III, and on the fractional populations based on the interproton NOEs. [g] Observed interproton distances. See footnotes *d* and *e*. [h] Observed Mn^{2+}–proton distances determined by paramagnetic effects on T_1 (Sloan & Mildvan, 1976).

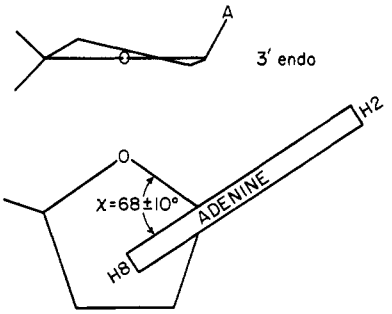

FIGURE 3: Conformation of MgATP bound at the secondary site (site 2) of pyruvate kinase, determined by the distance measurements in Table I.

(Figure 3) with a C5′–C4′–C3′–O3′ exocyclic torsional angle $\delta = 90 \pm 10°$. Although this combination of χ and δ is unusual, it is similar to the conformation of AMP bound at the active site of adenylate kinase (Fry et al., 1987).

The interproton distances in MgATP bound at site 1, the active site (Table I), could not be fit by a single nucleotide conformation. The reason is that the short distance from ribose H1′ to adenine H8 requires a contribution from a syn conformation while the similarly short distances from H2′ and H3′ to H8 require both high and low anti species. As was done in our previous analysis of the multiple conformations of free $Co(NH_3)_4ATP$ (Rosevear et al., 1983), a set of low-energy nucleotide conformations was chosen, on the basis of the observed grouping of structures found by X-ray analyses of purine ribonucleotides, and predicted by theoretical studies to be at or near energy minima (Saenger, 1984; deLeeuw et al., 1980; Berthod & Pullman, 1973; Yathindra & Sundaralingam, 1973; Levitt & Warshell, 1978). Models of a single representative conformation from each well-populated group were constructed, and interproton distances were measured in each model (Table II). The fractional contribution of each conformation (f_i) to the observed average interproton distances at site 1 ($\langle r_{AB} \rangle$ etc.) was calculated by simultaneous equations of the form

$$\langle r_{AB}^{-6} \rangle = f_I(r_{I,AB})^{-6} + f_{II}(r_{II,AB})^{-6} + f_{III}(r_{III,AB})^{-6} \quad (5)$$

$$\langle r_{CD}^{-6} \rangle = f_I(r_{I,CD})^{-6} + f_{II}(r_{II,CD})^{-6} + f_{III}(r_{III,CD})^{-6} \quad (6)$$

$$\langle r_{EF}^{-6} \rangle = f_I(r_{I,EF})^{-6} + f_{II}(r_{II,EF})^{-6} + f_{III}(r_{III,EF})^{-6} \quad (7)$$

$$\Sigma f_i = 1.0 \quad (8)$$

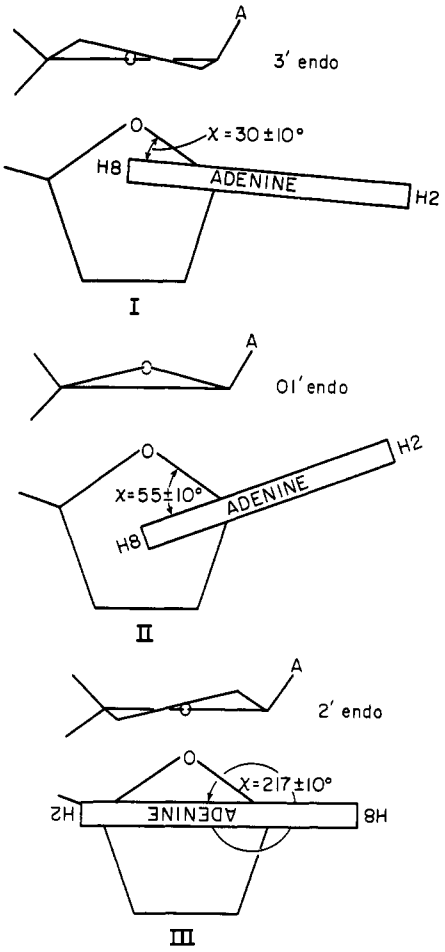

FIGURE 4: Conformations contributing to the structure of MgATP bound at the active site of pyruvate kinase, based on the distance measurements in Table I. The calculated fractional populations (Table II) are the following: conformation I, 62 ± 10%; conformation II, 20 ± 8%; conformation III, 18 ± 8%.

As previously found for free $Co(NH_3)_4ATP$ (Rosevear et al., 1983), no fewer than three stable nucleotide conformations were required to fit the interproton distances in MgATP at site 1 (Figure 4, Table II). The predominant conformation at site 1, contributing 62 ± 10% to the average, is a low-anti-3′-endo species. Smaller contributions from a high-anti-O1′-endo conformation (20 ± 8%) and from a syn-2′-endo conformation (18 ± 8%) were also required. This distribution

is similar to but not identical with that found for the adenine–ribose portion of free $Co(NH_3)_4ATP$ which could be fit by assuming 35 ± 11% low-anti-3′-endo, 44 ± 14% high-anti-O1′-endo, and 14 ± 5% syn-2′-endo (Rosevear et al., 1983). In the present case, it is clear that enzyme-bound MgATP is being detected since the NOEs were all negative and appeared within 0.5 s (Figure 2) and denaturation of the protein with 3.5 M guanidinium chloride removed all of the negative NOEs.

Comparison of MgATP Conformations at Site 1 Obtained by NOE and the Paramagnetic Probe–T_1 Method. Models of each of the three conformations of ATP used to fit the interproton distances at site 1 were built, and Mn^{2+} was placed at a position consistent with its measured distances from the α-, β-, and γ-phosphorus atoms (Sloan & Mildvan, 1976). Distances from Mn^{2+} to H8, H2, and H1′ were measured in each model and were averaged, by using equations of the form of eq 5–8, taking into account the fractional contribution of each conformation. The calculated average Mn^{2+}–proton distances (Table II) were consistent, within experimental error, with those measured at site 1 by the paramagnetic effects of enzyme-bound Mn^{2+} on the T_1 values of H8, H2, and H1′. The mutual consistency of the conformational populations of ATP bound at site 1 based on the measured interproton distances, and on the independently measured Mn^{2+} to proton distances, supports the validity of the analysis, although we cannot exclude the possibility that a different set of ATP conformations would also be consistent with the data. Regardless of the basis set chosen, the NOE data require multiple adenine–ribose conformations for MgATP bound at site 1.

Discussion

The multiple adenine–ribose conformations of MgATP bound at the active site of muscle pyruvate kinase, needed to fit the NOE measurements, and consistent with the paramagnetic probe–T_1 data, explain several previously observed properties of this enzyme. Pyruvate kinase has long been known to be relatively nonspecific in its utilization of purine and pyrimidine nucleotide substrates (Plowman & Krall, 1965), suggesting little or no interaction of the purine or pyrimidine rings with the protein (Mildvan, 1981). Mobility of the ethenoadenine ring of $Mg\epsilon ATP$[2] bound to pyruvate kinase was detected by fluorescence depolarization (Barrio et al., 1973). An X-ray study of the MgATP complex of cat muscle pyruvate kinase placed the adenine ring in a "large hydrophobic hole, not particularly specific for adenine" (Muirhead et al., 1986). Such conformational multiplicity of a bound nucleotide and nonspecificity of a nucleotide binding site are unusual in ATP-utilizing enzymes (Mildvan, 1981). These properties differ significantly from those of adenylate kinase (Fry et al., 1985) and protein kinase (Rosevear et al., 1983) which show high specificities for ATP and unique conformations of bound ATP. Similarly, in the MgdATP and MgTTP complexes of DNA polymerase I and its large fragment, unique nucleotide conformations and very high, template-directed specificities are observed (Sloan et al., 1975; Ferrin & Mildvan, 1985, 1986; Loeb & Kunkel, 1982). However, in the dGTP complex of DNA polymerase, two nucleotide conformations are required to fit the interproton distances; a low-anti, O1′-endo/C3′-endo species, which contributes 60 ± 5%, and a syn-C2′-endo species, which contributes 40 ± 5%. In the presence of a template, only the anti conformation is observed, suggesting that the introduction of specificity in DNA polymerase by the template restricts the conformational mobility of the nucleotide (Ferrin & Mildvan, 1986). As previously noted (Mildvan, 1981), from NMR and X-ray studies of several enzyme–nucleotide complexes, a unique and distorted nucleotide conformation correlates with high nucleotide base specificity of enzymes.

Detailed kinetic and substrate binding studies have revealed no catalytic or regulatory role for site 2, the secondary nucleotide binding site of muscle pyruvate kinase (Mildvan & Cohn, 1966). On the basis of the observations that pyruvate kinase enzymes from yeast and liver are allosterically activated by the effector FDP, site 2 of the muscle enzyme has been suggested to be a vestigial allosteric site which is no longer functional (Stuart et al., 1979). The present data, which detect a unique, and somewhat strained, high-anti-3′-endo conformation for MgATP bound at site 2, while implying specificity, clearly demonstrate that such properties of a bound ligand do not ensure functionality of the binding site.

References

Barrio, J. R., Secrist, J. A., Chien, Y., Taylor, P. J., Robinson, J. L., & Leonard, N. J. (1973) *FEBS Lett. 29*, 215–218.

Berthod, H., & Pullman, B. (1973) *FEBS Lett. 33*, 147–150.

Bücher, T., & Pfleiderer, G. (1955) *Methods Enzymol. 1*, 435–440.

de Leeuw, H. P. M., Haasnoot, C. A. G., & Altona, C. (1980) *Isr. J. Chem. 20*, 108–126.

Ferrin, L., & Mildvan, A. S. (1985) *Biochemistry 24*, 6904–6913.

Ferrin, L., & Mildvan, A. S. (1986) *Biochemistry 25*, 5131–5145.

Fry, D. C., Kuby, S. A., & Mildvan, A. S. (1985) *Biochemistry 24*, 4680–4694.

Fry, D. C., Kuby, S. A., & Mildvan, A. S. (1987) *Biochemistry 26*, 1645–1655.

Granot, J., Kondo, H., Armstrong, R. N., Mildvan, A. S., & Kaiser, E. T. (1979) *Biochemistry 18*, 2339–2345.

Kalk, A., & Berendsen, H. J. C. (1976) *J. Magn. Reson. 24*, 343–366.

Levitt, M., & Warshell, A. (1978) *J. Am. Chem. Soc. 100*, 2607–2613.

Loeb, L., & Kunkel, T. A. (1982) *Annu. Rev. Biochem. 52*, 429–457.

Melamud, E., & Mildvan, A. S. (1975) *J. Biol. Chem. 250*, 8193–8201.

Mildvan, A. S. (1981) *Philos. Trans. R. Soc. London, B 293*, 65–74.

Mildvan, A. S., & Cohn, M. (1965) *J. Biol. Chem. 240*, 238–246.

Mildvan, A. S., & Cohn, M. (1966) *J. Biol. Chem. 241*, 1178–1193.

Mildvan, A. S., & Gupta, R. K. (1978) *Methods Enzymol. 49G*, 322–359.

Mildvan, A. S., Granot, J., Smith, G. M., & Liebman, M. N. (1980) *Adv. Inorg. Biochem. 2*, 211–236.

Mildvan, A. S., Rosevear, P. R., Granot, J., O'Brian, C. A., Bramson, H. N., & Kaiser, E. T. (1983) *Methods Enzymol. 99*, 93–119.

Muirhead, H., Clayden, D. A., Barford, D., Lorimer, C. G., Fothergill-Gilmore, L. A., Schiltz, E., & Schmitt, W. (1986) *EMBO J. 5*, 475–481.

Noggle, J. H., & Schirmer, R. E. (1971) *The Nuclear Overhauser Effect*, pp 44–74, Academic Press, New York.

Plowman, K. M., & Krall, A. R. (1965) *Biochemistry 4*, 2809–2814.

Reynard, A. M., Hass, L. F., Jacobsen, D. D., & Boyer, P. D. (1961) *J. Biol. Chem. 236*, 2277–2283.

Rosevear, P. R., Bramson, H. N., O'Brian, C., Kaiser, E. T., & Mildvan, A. S. (1983) *Biochemistry 22*, 3439–3447.

Rosevear, P. R., Fox, T. L., & Mildvan, A. S. (1986) *Fed. Proc., Fed. Am. Soc. Exp. Biol. 45*, 1646.
Saenger, W. (1981) *Principles of Nucleic Acid Structure*, pp 51–104, Springer-Verlag, New York.
Sloan, D. L., & Mildvan, A. S. (1976) *J. Biol. Chem. 251*, 2412–2420.
Steinmetz, M. A., & Deal, W. C. (1966) *Biochemistry 5*, 1399–1405.
Stuart, D. I., Levine, M., Muirhead, H., & Stammers, D. K. (1979) *J. Mol. Biol. 134*, 109–142.
Tropp, J., & Redfield, A. G. (1981) *Biochemistry 20*, 2133–2140.
Wagner, G., & Wüthrich, K. (1979) *J. Magn. Reson. 33*, 675–680.
Yathindra, N., & Sundaralingam, M. (1973) *Biopolymers 12*, 297–314.

Structural Comparison of Acyl Carrier Protein in Acylated and Sulfhydryl Forms by Two-Dimensional ^{1}H NMR Spectroscopy†

Paul-James Jones, T. A. Holak, and J. H. Prestegard*
Department of Chemistry, Yale University, New Haven, Connecticut 06511
Received December 29, 1986

ABSTRACT: Sequence-specific assignments of ^{1}H NMR resonances are obtained for the backbone protons of *Escherichia coli* acyl carrier protein, acylated with an eight-carbon chain covalently attached to the prosthetic group thiol (octanoyl-ACP). Comparison of ^{1}H–^{1}H sequential connectivities in the NOESY spectra of octanoyl-ACP and the unacylated protein (ACPSH) indicates that secondary structure is largely conserved on acylation. Changes in resonance positions observed for certain groups of residues are interpreted in terms of a model that describes the spatial reorientation of secondary structural elements in the protein resulting from introduction of the acyl chain.

Acyl carrier proteins (ACPs)[1] are small, monomeric proteins that play an essential role in fatty acid biosynthesis for organisms with a type II fatty acid synthetase system. Although there is recent evidence for a more widespread function (Therisod et al., 1986), the accepted role of ACP is that of a shuttle, carrying the intermediates of fatty acid biosynthesis from site to site in the fatty acid synthetase system [for a review, see Vagelos (1973) and Volpe and Vagelos (1978)]. All ACPs studied are similar in that they are small (7.5–10 kDa), highly acidic proteins that have a 4'-phosphopantetheine prosthetic group. The intermediates of fatty acid biosynthesis are covalently attached to this group as acyl thio esters, and the prosthetic group is, in turn, covalently attached to the peptide backbone through a phosphodiester linkage to a serine side chain. Although the dominant view of ACP is that of a passive carrier, there is evidence to suggest that differences in the interaction of various acyl chains with a hypothetical binding site on ACP result in different enzyme affinities for these substrates and could be partly responsible for the fatty acid distribution produced by the synthetase system. For example, it is observed that thioesterase I is selective in the hydrolysis of palmitoyl- over *cis*-vaccenyl-ACPs, while it displays little selectivity when the corresponding acyl-CoAs serve as substrates (Barnes & Wakil, 1968; Spencer et al., 1978). Observations such as these have stimulated interest in the structural characterization of acyl-ACPs.

Among all known ACPs, the best characterized is that from *Escherichia coli*. This protein is quite representative of its class with 77 residues, with a large proportion (ca. 26%) of acidic residues, a much smaller proportion (ca. 8%) of basic residues, and a phosphopantetheine prosthetic group attached to Ser-36 (Majerus et al., 1965; Pugh & Wakil, 1965). The amino acid sequences of ACP from *E. coli* strains E-26 and K-12 are known (Vanaman et al., 1968a,b; S. Jackowski, J. E. Cronan, Jr., and C. O. Rock, personal communication). The sequence of strain B, the ACP used in this study, has been verified by NMR to be identical with that of strain E-26, with one exception, where Asp-24 is replaced by Asn (Holak & Prestegard, 1986). Although crystals yielding suitable diffraction data for ACP have been obtained (McRee et al., 1985), no crystal structure yet exists.

Recently, a secondary structural model for ACPSH has been proposed on the basis of interresidue contacts derived from analysis of two-dimensional nuclear Overhauser enhancement (NOE) data involving amide, α-, and β-protons (Holak & Prestegard, 1986). This structure agrees qualitatively with that previously proposed as the result of the application of the Chou–Fasman predictive algorithm (Rock & Cronan, 1979). Both proposals indicate a structure rich in α-helix, a conclusion further supported by earlier circular dichroism (Schulz, 1975) and optical rotary dispersion (Takagi & Tanford, 1968) studies. In the secondary structure de-

† This work was supported by a grant from the National Institutes of Health (GM 32243) and benefitted from instrumentation provided through shared instrumentation programs of the National Institute of General Medical Science (GM 32243S1) and the Division of Research Resources of NIH (RR02379).

[1] Abbreviations: ACP, acyl carrier protein; octanoyl-ACP, ACP with an eight-carbon acyl chain covalently attached to the prosthetic group thiol; ACPSH, ACP with a free prosthetic group thiol; RP-HPLC, reverse-phase high-pressure liquid chromatography; EDTA, ethylenediaminetetraacetic acid disodium salt; Tris, tris(hydroxymethyl)aminomethane; NMR, nuclear magnetic resonance; ppm, parts per million; NOE, nuclear Overhauser effect; COSY, two-dimensional J-correlated spectroscopy; relayed COSY, two-dimensional relayed coherence transfer spectroscopy; NOESY, two-dimensional NOE spectroscopy; d_{NN}, cross-relaxation connectivity between an amide proton and the amide proton on one of the neighboring residues; $d_{\alpha N}$, cross-relaxation connectivity between an amide proton and the α-proton of the preceding residue; $d_{\beta N}$, cross-relaxation connectivity between an amide proton and the β-proton(s) of the preceding residue.

0006-2960/87/0426-3493$01.50/0